Abdominal Radiology

Published online: 26 September 2018

Abdom Radiol (2019) 44:1027–1032
https://doi.org/10.1007/s00261-018-1787-6

Characterization of renal stone composition by using fast kilovoltage switching dual-energy computed tomography compared to laboratory stone analysis: a pilot study

Ukrit Rompsaithong,[1] Kantima Jongjitaree,[1] Pornpim Korpraphong,[2] Varat Woranisarakul,[1] Tawatchai Taweemonkongsap,[1] Chaiyong Nualyong,[1] and Ekkarin Chotikawanich[1]

[1]Division of Urology, Department of Surgery, Faculty of Medicine, Siriraj Hospital, Mahidol University, 2 Wanglang Road, Bangkoknoi, Bangkok 10700, Thailand
[2]Department of Radiology, Faculty of Medicine, Siriraj Hospital, Mahidol University, Bangkok, Thailand

Abstract

Purpose: To prospectively examine the diagnostic performance of fast kilovoltage switching dual-energy computed tomography (DECT) in characterization of in vivo renal stone composition compared with postoperative stone analysis.
Methods: Consecutive consenting patients scheduled for endoscopic kidney stone surgery in a tertiary referral hospital from June 2015 to January 2016 were enrolled. Patients were preoperatively scanned with single-source, fast kilovoltage switching DECT. Stone compositions were determined regarding the effective atomic number measurements. Results of the stone compositions from DECT were compared to postoperative infrared spectroscopy stone analysis as the standard reference.
Results: For the 39 patients enrolled in the study, DECT was able to detect uric acid stone with sensitivity of 88.9% and specificity of 100%. There was 100% positive predictive value, 96.8% negative predictive value, and 97.4% accuracy. For non-contrast CT scan, sensitivity was 88.9%, specificity was 96.7%, positive predictive value was 88.9%, negative predictive value was 96.7%, and accuracy was 94.8%. Of the 39 samples examined, 21 (54%) were single composition, whereas 18 (46%) were combined. Single composition stones were correctly characterized by DECT in 100% (8/8) for uric acid. Whereas the result of uric acid stone containing stone discrimination in mixed composition was not so good with Z_{eff} alone, iodine imaging can compensated this fault.
Conclusions: DECT provides excellent accuracy in characterizing uric acid stone compositions. With the addition of iodine image, all of uric acid-containing stones can be determined by the DECT.

Key words: Renal stone—Stone composition—Dual-energy computed tomography—Infrared spectroscopy

The incidence and prevalence of urolithiasis are increasing globally [1]. Moreover, renal stones are significant contributors to atrophic kidneys, causing persistent obstruction, chronic urinary tract infections, and scarring resulting in renal failure [2]. Regarding to treatment options, the two main categories of urinary stones are uric acid stone (17%), which does not require surgery, and non-uric acid stone (83%), which usually requires surgical treatment [3].

Pre-treatment determination of renal stone composition influences not only treatment plans such as urinary alkalinization used in uric acid stones and some types of stones that resist shock wave lithotripsy, but also stone recurrence prevention regimen. Especially for uric acid stone, treatment can be changed from surgical to non-surgical treatment that has low risk and cost for patients. Unfortunately, accurate determination of stone composition was only possible after extraction, therefore giving no benefits during preoperative treatment plans.

Correspondence to: Ekkarin Chotikawanich; *email:* ekkarinc@yahoo.com, ekkarin.cho@mahidol.ac.th

Although non-contrast computed tomography scanning (NCCT) is the standard investigation for diagnosing acute flank pain, and is also good for detecting stone location, size, and density measurement [4] in addition to predicting stone composition by using the CT number approach, it is not robust or reliable enough to be used as a routine clinical application [5].

Dual-energy computed tomography (DECT) has the ability to simultaneously operate two X-ray sources at different energy levels and provides the potential to differentiate between materials with similar electron densities but varying photon absorption rates, and therefore has the ability to distinguish stone components [6]. To date, most DECT studies have been performed on renal phantoms using ex vivo renal stones [7–10] and only a few in vivo studies with small study groups have been undertaken [11, 12].

In this study, a single-source fast kilovoltage switching second-generation DECT, a recent advance in scanning technology with the advantage of providing a full scan field of view (50 cm) and good temporal resolution, was used [13].

The objective of this study was to examine the diagnostic performance of fast kilovoltage switching DECT in characterization of in vivo renal stone composition compared with postoperative stone analysis methods.

Materials and methods

A pilot study, approved by Siriraj Institutional Review Board, protocol no. 062/2558 (EC1), was undertaken at Siriraj hospital, Mahidol University between June 2015 and January 2016. The inclusion criteria were consenting patients over 18 years old scheduled for percutaneous nephrolithotomy (PCNL) or retrograde intrarenal surgery (RIRS). Exclusion criteria were pregnancy and patients from whom stone retrieval for analysis was not possible.

Dual-energy computed tomography

Patients were preoperatively scanned with single-source fast kilovoltage switching DECT (Discovery CT750 HD, GE Healthcare, Milwaukee, WI, USA), equipped with 64 detectors and a 50-cm field of view. This system is capable of switching tube voltage between 80 and 140 kilovoltage peak (kVp) in less than 0.5 ms. After scout imaging examinations to limit area of interested, dual-energy CT scan was performed using spectral imaging (SI) mode (80/140 kVp tube voltage; 400 mA tube currents) in 1.25-mm-thick slices. Coronal and sagittal multiplanar reconstruction (MPR) images were also obtained.

Image evaluation

CT images were transferred to an Advantage workstation 4.6 (GE Healthcare, Milwaukee, WI, USA) for analysis using Gemstone Spectral Imaging (GSI), the renal stone analysis software package. Images were evaluated by a radiologist experienced in interpreting genitourinary system imaging, who was blind to the stone analysis results. In postprocedure processing, MPR imaging was made by data that obtained in 70 keV. Imaging details, including number of stone, stone location (upper, middle, lower, and renal pelvis), size (the largest dimension in both coronal and sagittal planes), and mean attenuation coefficient reported in Hounsfield unit, were recorded for all examinations. Regions of interest (ROI) were defined according to the largest possible area of each stone from a 1–2-mm boundary using axial imaging.

By applying two X-ray beam energies to a specified material, it is possible to calculate its effective atomic number (Z_{eff}) [14]. Thus, Z_{eff} can be used to characterize stone composition. However, on account of known differences in the chemical composition of various stone types, they can potentially have a unique Z_{eff} (Table 1). According to multi-composition of stone, therefore Z_{eff} of ROI was distributed into histogram and stone composition was determined at the maximum point of graph (Figs. 1C, 2C).

Regarding the material density images (MD), iodine (which has a high atomic number) and water (which has a low atomic number) images were selected as the basis pair because water and iodine span the atomic number range of materials generally found in CT imaging. The lower atomic number of uric acid stone preferentially causes Compton interaction with a low-energy beam, while there is minimal photoelectric interaction with the high-energy beam. Therefore, a stone visible on a water image but absent on an iodine image was characterized as uric acid stone (Fig. 1), whereas non-uric acid stones have higher atomic numbers and demonstrate both photoelectric and Compton interactions at both energies, and show brightly on both MD images (Fig. 2) [15].

Crystallography

Extracted stones were sent for crystallographic analysis and compositions were determined using Fourier transform infrared (FTIR) spectroscopy.

Pure stones were defined as those composed of only one substance (100%) and mixed stones were defined as

Table 1. Effective atomic number (Z_{eff}) of common urinary stone types

Urinary stones	Z_{eff}
Uric acid	6.95
Struvite	9.74
Cystine	11.15
Calcium oxalate monohydrate	13.32
Calcium oxalate dihydrate	13.80
Calcium phosphate	15.99

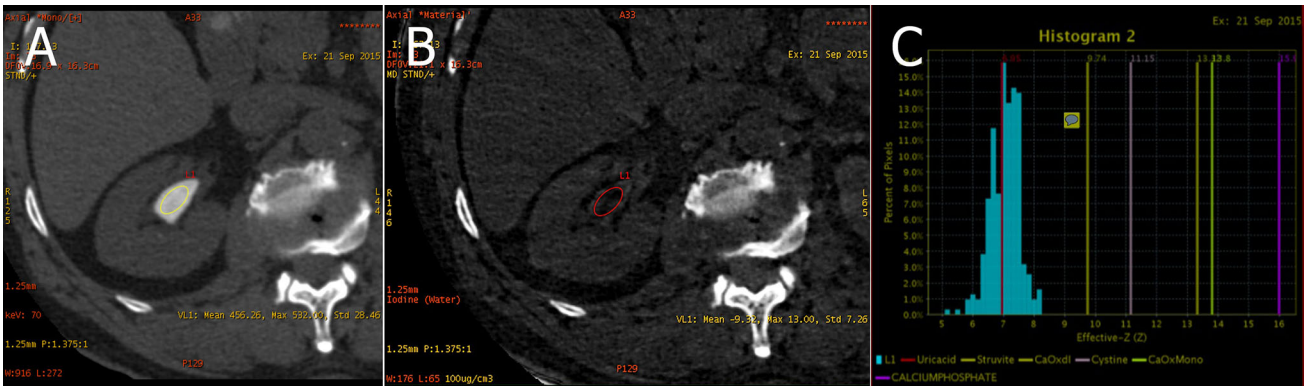

Fig. 1. Uric acid stone, axial DECT. **A** (Left) 70-keV water image. **B** (Middle) Iodine image—kidney stone, which is seen in water images but not seen with iodine image suggested uric acid stone. **C** (Right) Histogram of percentage of pixels of effective atomic number, peak of histogram consistent with uric acid stone.

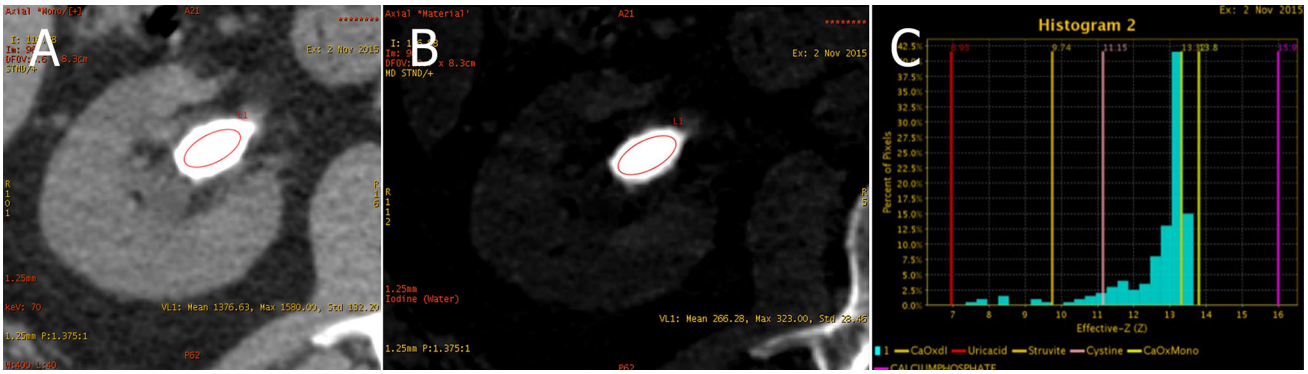

Fig. 2. Non-uric acid stone (Calcium oxalate 70%, calcium phosphate 30%), axial DECT. **A** (Left) 70-keV water image. **B** (Middle) Iodine-density image—kidney stone, which is seen in both water and iodine image suggested non-uric containing stone. **C** (Right) Histogram of percentage of pixels of effective atomic number, peak of histogram consistent with calcium oxalate stone.

those with one substance comprising more than 50% of the whole.

Radiation dose

Radiation dose in volume CT dose index (CTDIvol, mGy), dose-length product (DLP, mGy-cm), and acquisition length in millimeter was recorded for each patient. Effective radiation dose (mSv) was calculated by DLP × Effective factor (0.015 for abdomen CT) for each patient. According to radiation safety protocol, this study limited CTDIvol at 10.76 mGy similar to non-contrast abdominal CT imaging.

Statistical analysis

Statistical analysis was performed using SPSS version 20 software (Chicago, IL, USA). Continuous variables were presented in mean ± SD. Categorical variables were presented in frequencies or percentages.

The results of stone compositions according to the effective atomic number measurement and iodine image were compared to infrared spectroscopy stone analysis using diagnostic performance study (sensitivity, specificity, positive predictive value, negative predictive value, and accuracy).

Results

Thirty-nine patients were enrolled, including 24 female and 15 male patients. The mean age was 56 years old (range 29–73 years). Twenty-three patients underwent retrograde intrarenal surgery (RIRS), whereas 16 underwent percutaneous nephrolithotomy (PCNL).

The majority of patients had opaque, homogeneous stones (Table 2). The mean stone area was 277.4 mm^2 (33.7–1001.5 mm^2). The mean attenuation coefficient was 980.38 HU (412.42–1503.81 HU) (Table 3).

Stone compositions characterized by FTIR consisted of 21 (54%) pure stones (8 uric acid stones, 7 calcium oxalate stones, 5 calcium phosphate stones, 1 struvite

Table 2. Stone characteristics

Parameters	N	Percent
Side		
Right	24	61.5
Left	15	38.5
Opacity		
Opaque	29	74.4
Semi-opaque	9	23.1
Non-opaque	1	2.6
Location		
Upper calyx	2	5.1
Middle calyx	6	15.4
Lower calyx	10	25.6
Pelvic stone	10	25.6
Staghorn	11	28.2
Homogenous	34	87.2
Heterogenous	5	12.8

stone) and 18 (46%) mixed stones (1 uric acid stone, 11 calcium oxalate stones, 6 calcium phosphate stones). No cystine stones were present in our study (Table 4).

Based on Z_{eff}, discrimination of uric acid from non-uric acid (calcium oxalate, calcium phosphate, struvite) stones had a sensitivity of 88.9% (8/9), specificity of 100% (30/30), positive predictive value of 100% (8/8), negative predictive value of 96.8% (30/31), and accuracy of 97.4% (38/39) as shown in Table 5. To evaluate uric acid stone by Hounsfield unit, which determined uric acid stone at 200–600 HU [15], there were sensitivity of 88.9% (8/9), specificity of 96.7% (29/30), positive predictive value of 88.9% (8/9), negative predictive value of 96.75%(29/30), and accuracy of 94.8% (37/39) as shown in Table 6.

Pure stones were correctly characterized by Z_{eff} in 100% (8/8) of uric acid and 85% (6/7) of calcium oxalate stones; however, calcium phosphate (0/5) and struvite stones (0/1) were not correctly identified. Of the 18 stones with mixed compositions, 72.7% (8/11) of calcium oxalate stones were correctly characterized, whereas uric acid (0/1) and calcium phosphate stones (0/6) were not identified (Table 7). Furthermore, the addition of MD, particularly iodine image could determine all of the uric acid stones.

Mean BMI in this study was 26.0 kg/m^2(17.4–45.2 kg/m^2). Mean stone size was 277.4 mm^2 (33.7–1001.5 mm^2). One patient (BMI = 27.6 kg/m^2 and stone size = 56.27 mm^2) who had mixed uric acid stone was characterized as non-uric acid stone preoperatively, while others were correctly characterized.

Table 4. Stone compositions

Stone composition	N
Pure stone	21
Uric acid	8
Calcium oxalate	7
Calcium phosphate	5
Struvite	1
Mixed stone	18
Uric acid	1
Calcium oxalate	11
Calcium phosphate	6
Total	39

Pure stones: composed with only one component (100%)
Mixed stones: one component comprising more than 50% of the whole

Table 5. Overall discrimination of uric from non-uric acid stone by DECT (using Z_{eff})

	N/N	Value (%)	95% CI (%)
Sensitivity	8/9	88.9	56.5–99
Specificity	30/30	100	88.5–100
Positive predictive value	8/8	100	67.6–100
Negative predictive value	30/31	96.8	82.5–99.5
Accuracy	38/39	97.4	86.5–99.9

Table 6. Overall discrimination of uric from non-uric acid stone by DECT (using HU)

	N/N	Value (%)	95% CI
Sensitivity	8/9	88.9	51.6–99.7
Specificity	29/30	96.7	82.8–99.9
Positive predictive value	8/9	88.9	53.5–98.2
Negative predictive value	29/30	96.7	82.0–99.5
Accuracy	37/39	94.8	82.7–99.4

Discussion

Numerous in vitro and a few in vivo studies demonstrated that first-generation dual-source DECT had excellent results with high sensitivity and specificity in differentiating uric acid from non-uric acid stones and few of the non-uric acid stone types [5, 8, 9, 12]. The

Table 3. Stone attenuation coefficient for different groups of stones

Stone composition	N	Mean (HU)	Minimum (HU)	Maximum (HU)	SD
Uric acid	9	484.37	412.42	620.00	62.39
Struvite	1	735.75	735.75	735.75	–
Calcium oxalate	17	1124.19	643.50	1464.21	267.69
Calcium phosphate	12	1169.06	455.77	1503.81	286.25
Total	39	980.38	412.42	1503.81	367.49

HU, Hounsfield unit

Table 7. Correctly characterized pure stone and mixed stone by effective atomic number

Stone composition	N	Percent
Pure stone	21	
Uric acid	8/8	100%
Calcium oxalate	6/7	85.7%
Calcium phosphate	0/5	0%
Struvite	0/1	0%
Mixed stone	18	
Uric acid	0/1	0%
Calcium oxalate	8/11	72.7%
Calcium phosphate	0/6	0%

smaller field of view (20–33 cm) for one X-ray tube precluded DECT applications in very large patients, which was considered a profound limitation [5, 8, 12, 15]. However, stone that is centrally located could be included in the smaller field of view.

In this study, we used a single-source DECT, which has a single X-ray tube with a full 50-cm field of view and fast scintillator gemstone detector, capable of rapidly switching tube voltage between 80 and 140 kVp in less than 0.5 ms, enabling simultaneous displays for review of conventional low/high kVp HU attenuation, material density, and effective Z images [16]. Previous studies suggested that HU and their variants are useful for predicting the composition of stones. However, they proved insufficient for certain types of stone as there was an overlap between HU values, especially for mixed stones [17, 18]. In our study, 18 (46%) of 39 patients had mixed stones. Mean HU ± SD of uric acid was 484.37 ± 62.39, struvite was 735.75, calcium oxalate was 1124.19 ± 267.69, and calcium phosphate was 1169.06 ± 286.25, showing that despite having the same order as Z_{eff}, there was an overlap between the HU values. The study also revealed accuracy for differentiating uric and non-uric component when using HU was 94.8% (Table 6) compared to using Z_{eff} in which the accuracy was 97.4% (Table 5).

Our study demonstrates DECT ability in an in vivo setting, showing that it can effectively differentiate between uric and non-uric acid stones based on Z_{eff} with sensitivity and specificity of 88.9% (8/9) and 100% (30/30), respectively. Using Z_{eff} alone was able to characterize all pure uric acid stone but unable to detect one mixed uric acid stone, which has 60% uric acid and 40% calcium oxalate. The improved results with DECT were when using material density images which correctly characterized ''one'' mixed composition uric acid stone that was incorrectly characterized on the other two techniques. Manglaviti et al. evaluated in vivo stone composition in 40 patients, concluding that DECT showed excellent accuracy in classifying urinary stone composition but failed to identify 4 stones with mixed composition [19]. The difficulty of correctly identifying mixed stone composition is probably related to stone cores which may not truly represent the ROI especially in heterogeneous stones. Our study failed to identify all of the calcium phosphate stones (0/11) and struvite stone (0/1), presumably from the heterogeneity, the high percentage of mixed stones, and different calcium phosphate chemical formulae and atomic numbers (for example carbonate apatite, calcium hydroxyapatite, or brushite stones). Another limitation was the relatively small patient population, which included only one patient with a pure struvite stone and no patients with cystine stones.

Radiation exposure of patients during imaging for stone detection is a concerning issue. In this study, radiation was limited to CDTIvol at 10.76 mGy, while the accuracy to discriminate uric from non-uric acid stone was 97.4%; however, the accuracy was improved to 100% when combine with iodine imaging. Kulkarni reported the accuracy to discriminate uric from non-uric acid stone was 100% when using DECT with CDTIvol at 19.11 mGy and the accuracy was 69% when using low-dose CT scan with CDTI vol at 5.14 mGy [20]. Mean BMI in this study was 26 kg/m^2 (17.4–45.2 kg/m^2), and our study was unable to characterize uric from non-uric acid stone in a patient with BMI of 27.6 kg/m^2. However, this patient had mixed uric acid stone that may be the cause of failure to characterize, and therefore our study was unable to conclude the correlation between the accuracy and BMI.

In conclusion, DECT using Z_{eff} provides excellent result in characterizing uric acid stone with high sensitivity (88.9%), high specificity (100%), and high accuracy (97.4%). With the addition of iodine images, all uric acid-containing stones can be determined by DECT.

Acknowledgments The authors gratefully acknowledge Ms. Chulaluck Boonma and Mr. Weerachat Churawd for their assistances of the data analysis and research processes, respectively.

References

1. Romero V, Akpinar H, Assimos DG (2010) Kidney stones: a global picture of prevalence, incidence, and associated risk factors. Rev Urol 12(2–3):e86–e96
2. Rule AD, Bergstralh EJ, Melton LJ 3rd, et al. (2009) Kidney stones and the risk for chronic kidney disease. Clin J Am Soc Nephrol 4(4):804–811
3. Johri N, Cooper B, Robertson W, et al. (2010) An update and practical guide to renal stone management. Nephron Clin Pract 116(3):c159–c171
4. Bultitude M, Smith D, Thomas K (2016) Contemporary management of stone disease: the new EAU urolithiasis guidelines for 2015. Eur Urol 69(3):483–484
5. Primak AN, Fletcher JG, Vrtiska TJ, et al. (2007) Noninvasive differentiation of uric acid versus non-uric acid kidney stones using dual-energy CT. Acad Radiol. 14(12):1441–1447
6. Flohr TG, McCollough CH, Bruder H, et al. (2006) First performance evaluation of a dual-source CT (DSCT) system. Eur Radiol. 16(2):256–268
7. Ferrandino MN, Pierre SA, Simmons WN, et al. (2010) Dual-energy computed tomography with advanced postimage acquisition data processing: improved determination of urinary stone composition. J Endourol 24(3):347–354

8. Graser A, Johnson TR, Bader M, et al. (2008) Dual energy CT characterization of urinary calculi: initial in vitro and clinical experience. Investig Radiol 43(2):112–119
9. Boll DT, Patil NA, Paulson EK, et al. (2009) Renal stone assessment with dual-energy multidetector CT and advanced postprocessing techniques: improved characterization of renal stone composition–pilot study. Radiology. 250(3):813–820
10. Li X, Zhao R, Liu B, Yu Y (2013) Gemstone spectral imaging dual-energy computed tomography: a novel technique to determine urinary stone composition. Urology. 81(4):727–730
11. Hidas G, Eliahou R, Duvdevani M, et al. (2010) Determination of renal stone composition with dual-energy CT: in vivo analysis and comparison with X-ray diffraction. Radiology. 257(2):394–401
12. Stolzmann P, Kozomara M, Chuck N, et al. (2009) In vivo identification of uric acid stones with dual-energy CT: diagnostic performance evaluation in patients. Abdom Imaging. 35(5):629–635
13. Mansouri M, Aran S, Singh A, et al. (2015) Dual-energy computed tomography characterization of urinary calculi: basic principles, applications and concerns. Curr Probl Diagn Radiol 44(6):496–500
14. Krasnicki T, Podgorski P, Guzinski M, et al. (2012) Novel clinical applications of dual energy computed tomography. Adv Clin Exp Med 21(6):831–841
15. Sheir KZ, Mansour O, Madbouly K, et al. (2005) Determination of the chemical composition of urinary calculi by noncontrast computerized tompography. Urol Res. 33:99–104
16. Kaza RK, Platt JF, Cohan RH, et al. (2012) Dual-energy CT with single- and dual-source scanners: current applications in evaluating the genitourinary tract. Radiographics. 32(2):353–369
17. Gucuk A, Uyeturk U (2014) Usefulness of hounsfield unit and density in the assessment and treatment of urinary stones. World J Nephrol 3(4):282–286
18. Zilberman DE, Ferrandino MN, Preminger GM, et al. (2010) In vivo determination of urinary stone composition using dual energy computerized tomography with advanced post-acquisition processing. J Urol 184(6):2354–2359
19. Manglaviti G, Tresoldi S, Guerrer CS, et al. (2011) In vivo evaluation of the chemical composition of urinary stones using dual-energy CT. AJR 197(1):W76–W83
20. Kulkarni NM, Eisner BH, Pinho DF, et al. (2013) Determination of renal stone composition in phantom and patients using single-source dual-energy computed tomography. J Comput Assist Tomogr 37(1):37–45